Brief Communication

MOLECULAR METABOLISM

Testosterone metabolites differentially regulate obesogenesis and fat distribution

Zachary L. Sebo [1], Matthew S. Rodeheffer [1,2,3,4,5,*]

ABSTRACT

Objective: Low testosterone in men (hypogonadism) is associated with obesity and type II diabetes. Testosterone replacement therapy has been shown to reverse these effects. However, the mechanisms by which testosterone regulates total fat mass, fat distribution, and metabolic health are unclear. In this study, we clarify the impact of hypogonadism on these parameters, as well as parse the role of testosterone from its downstream metabolites, dihydrotestosterone (DHT), and estradiol, in the regulation of depot-specific adipose tissue mass.

Methods: To achieve this objective, we utilized mouse models of male hypogonadism coupled with hormone replacement therapy, magnetic resonance imaging (MRI), glucose tolerance tests, flow cytometry, and immunohistochemical techniques.

Results: We observed that castrated mice develop increased fat mass, reduced muscle mass, and impaired glucose metabolism compared with gonadally intact males. Interestingly, obesity is further accelerated in castrated mice fed a high-fat diet, suggesting hypogonadism increases susceptibility to obesogenesis when dietary consumption of fat is elevated. By performing hormone replacement therapy in castrated mice, we show that testosterone impedes visceral and subcutaneous fat mass expansion. Testosterone-derived estradiol selectively blocks visceral fat growth, and DHT selectively blocks the growth of subcutaneous fat. These effects are mediated by depot-specific alterations in adipocyte size. We also show that high-fat diet-induced adipogenesis is elevated in castrated mice and that this can be rescued by androgen treatment. Obesogenic adipogenesis is also elevated in mice where androgen receptor activity is inhibited.

Conclusions: These data indicate that hypogonadism impairs glucose metabolism and increases obesogenic fat mass expansion through adipocyte hypertrophy and adipogenesis. In addition, our findings highlight distinct roles for testosterone, DHT, and estradiol in the regulation of total fat mass and fat distribution and reveal that androgen signaling blocks obesogenic adipogenesis in vivo.

Keywords Obesity; Diabetes; Testosterone; Fat distribution; Adipogenesis

1. INTRODUCTION

Low testosterone in men, known as hypogonadism, is associated with reduced muscle mass [1,2] and an increased incidence of obesity and diabetes [3–6]. Although the role of testosterone in maintaining muscle mass in males is well established [7–9], how testosterone exerts its anti-obesogenic effects is less clear. Testosterone is an agonist of the androgen receptor (AR) and a pro-hormone capable of being converted to the more potent androgen, dihydrotestosterone (DHT), or estradiol by 5a-reductase and aromatase, respectively. DHT cannot be aromatized to estradiol as testosterone can and exerts its biological effects through AR; estradiol does so through estrogen receptors (ERs) and GPR30 [10,11]. Androgens and estrogens are thought to mediate anti-obesogenic processes. For example, testosterone and DHT have been shown to inhibit adipogenesis in vitro [12–14], and testosterone replacement therapy reduces adiposity in hypogonadal men and mice [15,16]. However, data involving the role of DHT in fat mass regulation in vivo are conflicting. DHT treatment of hypogonadal males has been shown to decrease fat mass [17], have little to no effect on adiposity [15,16], and promote fat mass expansion [18].

By contrast to DHT, estradiol has consistently been observed to negatively regulate fat mass. For example, treating gonadally intact male mice with estradiol impedes excessive fat mass expansion when animals are fed a high-fat diet (HFD) [19], and ERα knockout male mice develop obesity [20]. Aromatase knockout mice, which do not convert testosterone to estradiol, also develop obesity [21,22], and a deleterious mutation in the aromatase gene of a man resulted in excessive adipose tissue and metabolic complications [23]. Therefore, the conversion of testosterone to estradiol by aromatase is likely important for impeding fat mass expansion in males. However, the role of estradiol in the regulation of male fat distribution is less clear.

Under normal conditions, men are known to accrue a proportionally greater quantity of visceral fat than women do, who accrue more subcutaneous fat than men do [24]. However, after menopause, when estradiol levels decrease, women progressively develop a more masculine fat distribution [25] that can be slowed by estradiol treatment [26]. Whether estradiol reduces visceral fat storage, enhances

[1]Yale University, Department of Molecular, Cellular and Developmental Biology, USA [2]Department of Comparative Medicine, Yale University, USA [3]Department of Physiology, Yale University, USA [4]Yale Stem Cell Center, USA [5]Yale Program in Integrative Cell Signaling and Neurobiology of Metabolism, USA

*Corresponding author. Comparative Medicine, Yale University School of Medicine, 375 Congress Ave, New Haven, CT, 06520, USA. Fax: +203 785 7499. E-mail: matthew.rodeheffer@yale.edu (M.S. Rodeheffer).

Received August 11, 2020 • Revision received November 20, 2020 • Accepted December 3, 2020 • Available online 9 December 2020

https://doi.org/10.1016/j.molmet.2020.101141

storage in subcutaneous depots, or both remains unclear. By contrast, treating hypogonadal men with testosterone has been shown to preferentially reduce either visceral [27,28] or subcutaneous fat stores [29,30], and a role for DHT in fat distribution has not been reported. Thus, fat distribution in males may be influenced by the combined effects of testosterone, DHT, and estradiol. In this study, we leveraged pharmacologic approaches and mouse models of male hypogonadism to clarify the role of testosterone metabolism in the regulation of body composition, fat distribution, and metabolic disease.

2. MATERIALS AND METHODS

2.1. Animal models

Experiments were approved by the Yale Institutional Animal Care and Use Committee. ARdY mice [31](Stock #001809) and mTmG mice [32](Stock #007576) were acquired from the Jackson Laboratory. The *eda* mutation was bred out of the ARdY strain before initiating experiments. ARdY:mTmG mice were generated by breeding AR mutant heterozygous females with mTmG+ males. Castrated C57Bl/6J mice were also acquired from the Jackson Laboratory. Surgery was performed at 3 weeks of age. HFD was 60% lard from Research Diets (D12492) and a standard diet from Harlan Laboratories (2018S). Hormonal and drug treatments were administered by using Alzet miniosmotic pumps (model #1004). Alzet pumps were made compatible with MRI by replacing the stainless-steel flow moderator with PEEK medical microtubing (DURECT Corporation #0002612). Vehicle was 45% w/v 2-hydroxypropyl-β-cyclodextrin (Cayman Chemical #16169) in 1X PBS or 45% w/v 2-hydroxypropyl-β-cyclodextrin (Cayman Chemical #16169) in 1X PBS + 10% DMSO (Sigma Aldrich #D5879). Testosterone (Cayman Chemical #15645) and DHT (Cayman Chemical #15874) were dosed at 2 mg/kg body weight/day and estradiol (Cayman Chemical #10006325) at 2 ug/kg body weight/day. Letrozole (Cayman Chemical #11568) was dosed at 0.4 mg/kg body weight/day, and bicalutamide (Cayman Chemical #14250) and dutasteride (Cayman Chemical #15956) at 0.5 mg/kg body weight/day. Notably, the bicalutamide dosage used here was 25%–30% of the dose commonly used for men with locally advanced prostate cancer [33,34].

2.2. Glucose metabolism, body composition, and fat distribution

Glucose tolerance tests (GTTs) were performed by fasting animals overnight (16–18 h). Next, we determined the fasting blood glucose level via a tail vein nick. A 20% glucose solution in saline was then injected intraperitoneally at a concentration of 2 g glucose/kg body weight. Blood glucose level was assessed 10, 20, 30, 60, and 120 min after glucose injections. Glucose tolerance refers to the incremental area under the curve (iAUC). Body composition (i.e., lean and fat mass) was determined for each mouse by using MRI (EchoMRI-100H, EchoMRI, Houston, TX, USA). Fat distribution was calculated according to the following equation:

$$\log10(\frac{SWAT}{VWAT})$$

In this equation, SWAT = inguinal subcutaneous fat mass (g) and VWAT = perigonadal visceral fat mass (g). The logarithm is taken from the SWAT/VWAT ratio to correct for skew.

2.3. Adipocyte hypertrophy and hyperplasia

To quantify adipocyte size (hypertrophy), adipose tissue was paraffin embedded for histological analysis, as previously described [35]. Next, 5 um sections were trichrome stained and imaged at 20X on a Keyence BZ-X800 microscope. A described pipeline in Cell Profiler [36] was used to determine adipocyte size [35]. The size of at least 100 adipocytes was averaged for each biological replicate. New adipocyte formation (hyperplasia) occurs in response to HFD feeding and occurs in 2 stages. In the first stage, adipose-resident adipocyte precursors (APs) proliferate during the first week of HFD feeding. In the second stage, proliferative APs from stage 1 differentiate into new adipocytes over the course of 7 weeks [37]. New adipocyte formation was quantified by initiating animals on an HFD while treating them with 0.4 mg/ml BrdU in their drinking water for 1 week. BrdU is a thymidine analog and is incorporated into the DNA of proliferating cells during the S phase of the cell cycle.

After 1 week, BrdU was removed from the drinking water, and animals were kept on a HFD for 7 weeks to allow APs to differentiate into adipocytes. Adipose tissue was paraffin embedded and sectioned as described. Sections were deparaffinized, rehydrated, and then underwent antigen retrieval in 10 mM sodium citrate (pH 6.0) in a 2100 Retriever (PickCell laboratories). Sections were blocked and stained in 2% BSA PBS. Sections were incubated in rabbit anti-Caveolin (Cell Signaling #3238; 1:400 dilution) and rat anti-BrdU (Abcam #ab6326; 1:300 dilution) primary antibodies overnight at 4C.

The next day, sections were washed in 2% BSA PBS and incubated in secondary antibodies for 4 h at room temperature in the dark. Secondary antibodies were goat anti-rabbit rhodamine-x-red (Jackson ImmunoResearch 111-295-144; 1:400 dilution) and goat anti-rat-A488 (Jackson ImmunoResearch 112-545-167; 1:400 dilution). Slides were mounted with DAPI Flouromount-G (Southern Biotech) and imaged with a Leica SP5 confocal microscope. At least 100 BrdU+ adipocyte nuclei were counted for each biological replicate.

To quantify AP proliferation, animals are fed an HFD and given 0.8 mg/ml BrdU in their drinking water for 1 week. After this treatment, animals were sacrificed and the adipose tissue was harvested. Adipose tissue was minced and digested in 1X HBSS (Gibco Cat# 14185052) supplemented with 3% BSA (AmericanBio 9048-46-8), 0.8 mM $ZnCl_2$, 1.0 mM $MgCl_2$, 1.2 mM $CaCl_2$ and 0.8 mg/ml Collagenase Type 2 (Worthington) in a shaking water bath (130 rpm) at 37 °C. After digestion, homogenate was filtered through a 40 um cell filter and centrifuged at 300 g for 3 min. The pellets were then resuspended in 1 ml of 1x HBSS + 3% BSA to wash the cells and transferred to a 1.5 ml Eppendorf tubes before centrifugation at 300 *g* for 3 min.

Next, the cell pellets were resuspended in 50 ul of 1x HBSS + 3% BSA with the following antibodies: CD29-A700 (BioLegend, 102218; 1:400 dilution), CD31-PECy7 (eBioscience, 25-0311-82, clone 390; 1:500 dilution), Sca1-Pacific Blue (BD Biosciences, 560653, clone D7; 1:250 dilution), and CD45-APC e780 (eBioscience; 47-0451-80, clone 30-F11; 1:500 dilution) for 30 min on ice in the dark. Cells were then washed in PBS, followed by fixation and permeabilization by Phosflow Lyse/Fix (Cat# 558049) and Perm Buffer III (Cat# 558050) (BD Biosciences) according to the manufacturer's instructions. The cells were pelleted and then washed in PBS with Ca and Mg, followed by treatment with DNase (Worthington; 1mg/10 ml) for 90 min at 37 °C in a water bath with gentle agitation (50 rpm) in the dark. Cells were pelleted and washed in 3% BSA + 1x HBSS followed by overnight incubation at 4 °C in the dark in anti-BrdU antibody (Alexa Fluor 647; Phoenix Flow Systems; AX647, clone PRB-1; 1:30 dilution).

The next day, the cells were washed in 3% BSA + 1x HBSS and incubated in the following antibodies for 1 h at room temperature in the dark: CD24-PerCPCy5.5 (eBioscience, 45-0242-80, clone M1/69; 1:200 dilution), CD34-PE (BioLegend, clone MEC14.7; 1:400 dilution), CD29-A700 (BioLegend, 102218; 1:400 dilution), CD31-PECy7 (eBioscience, 25-0311-82, clone 390; 1:500 dilution), Sca1-Pacific Blue (BD Biosciences, 560653, clone D7; 1:250 dilution), and CD45-

APC e780 (eBioscience; 47-0451-80, clone 30-F11; 1:500 dilution). After antibody incubation, cells were washed in 3% BSA + 1x HBSS, and BrdU+ APs were identified by using flow cytometry. For the ARdY to male adipocyte precursor AP transplants, APs were isolated via FACS and 500,000–1,000,000 cells were injected into the inguinal subcutaneous fat pad of 3–6-week-old male mice. After a 2-week recovery period, mice were given an HFD and 0.8 mg/ml BrdU in their drinking water to mark proliferative cells. Because ARdY cells were mTmG+, Sca1-Pacific Blue was replaced with Sca1-V500 (BD Horizon, 561228, clone D7; 1:250 dilution) and CD34-PE was replaced with CD34-BV 421 (BioLegend 119321, clone MEC14.7; 1:400 dilution).

2.4. mRNA expression

Gene	Primer Sequence (5′→3′)
Androgen Receptor	Forward: CCTTATGGGGACATGCGTTTG
	Reverse: CCCAGAGTCATCCCTGCTTC
MED1 (reference gene)	Forward: AATAGACCTTTCACCCCACCT
	Reverse: CCCACCATCACTGTCCCTTTA
TBK1 (reference gene)	Forward: ACTGGTGATCTCTATGCTGTCA
	Reverse: TTCTGGAAGTCCATACGCATTG
Adiponectin (control)	Forward: GGAGATGCAGGTCTTCTTGG
	Reverse: GCGATACACATAAGCGGCTTC

All samples were run in technical duplicate or triplicate on a LightCycler 480 instrument. Relative gene expression was determined by using the standard curve method. Reference gene expression is shown in (Supp. Fig. 3A–C). To confirm the separation of adipocytes from stomal vascular cells in adipose tissue, adiponectin expression was determined (adipocytes = adiponectin+; SVC = adiponectin-; Supp. Fig. 3D).

2.5. Statistical analysis

Statistical tests were performed using GraphPad Prism version 8.0 and are denoted in figure legends. Data are presented as mean ± SEM, and $p < 0.05$ was considered statistically significant. For multiple linear regression analysis, diet, hormonal status (castration vs. sham), and body composition parameter (i.e., body weight, lean mass, or fat mass) were considered independent variables. Analyses were parsed according to body composition parameter to account for multicollinearity among these datasets, and structural multicollinearity was reduced by centering the independent variables.

3. RESULTS

3.1. Hypogonadism alters body composition, impairs glucose metabolism, and accelerates diet-induced obesity

Castrated rodents and other mammals are commonly used to model hypogonadism in men because this procedure dramatically reduces testosterone levels [38] and accurately recapitulates the changes in body composition observed in hypogonadal men, namely, increased fat mass and decreased lean mass [16,39,40]. Lean mass is predominately muscle, the major site of glucose uptake [41]. Lower muscle mass is associated with impaired glucose metabolism in patients with and without diabetes [42–44]. Excessive adipose tissue mass contributes to metabolic disease risk in obesity [45].

To determine the impact of hypogonadism on body composition and glucometabolic health, we fed castrated and sham mice a standard diet (SD) or HFD for 8 weeks followed by assessments of body composition and glucose metabolism. Castrated mice weighed less than sham mice on an SD, but total body weight was the same between the castrated and sham animals on an HFD (Figure 1A). Castrated mice developed more fat mass and less lean mass than did sham controls on both diets (Figure 1B,C). However, the rate of fat gain was more pronounced on the HFD in castrated mice (Supp. Fig. 1A, B), indicating that hypogonadism further accelerates obesity development when dietary fat intake is high. The increased fat mass is accounted for by a greater quantity of both visceral and subcutaneous fat (Figure 1D–F). On an SD, castrated animals displayed elevated fasting glucose, but glucose tolerance was the same as that of sham controls (Figure 2A,C). On an HFD, however, fasting glucose and glucose intolerance were significantly elevated in castrated mice (Figure 2B,D). By using multiple linear regression analysis, we observed that diet and hormonal status (castration vs. sham), rather than body composition parameters, are the major determinants of glucometabolic health. However, fat mass exhibits considerable multicollinearity with diet (Supp. Table 1), which was expected because HFD feeding promotes obesity. Taken together, these data support the notion that hypogonadism in males impairs glucose metabolism, reduces lean mass, and promotes the expansion of adipose tissue. Given that castration further accelerates obesity development on an HFD (Supp. Fig. 1A, B), we attempted to determine the cellular mechanisms by which testosterone and its metabolites regulate fat mass.

3.2. Testosterone metabolites incur depot specificity to adipocyte hypertrophy

To identify specific roles of testosterone, estradiol, and DHT in regulating total fat mass and fat distribution, we treated distinct cohorts of castrated mice with one of these hormones each in addition to feeding them an HFD for 4 weeks. Because castration dramatically reduces androgens and estrogens [46], adding back individual hormones will allow the identification of their unique role in regulating obesogenic fat mass expansion. As expected, testosterone effectively reduced HFD-induced fat mass expansion (Figure 3A). DHT treatment, however, had no effect on fat gain on an HFD (Figure 3B). By contrast, treating castrated mice with estradiol modestly ameliorated HFD-induced obesogenesis (Figure 3C). Consistently, treating gonadally intact male mice with the aromatase inhibitor (AI), letrozole, resulted in a greater accumulation of fat than in vehicle-treated controls (Figure 3D), despite an apparent increase in androgen levels as a readout by elevated seminal vesicle mass (Supp. Fig. 1C). These data support findings that have indicated that the anti-obesogenic activity of testosterone in males is at least partly mediated by its conversion to estradiol by aromatase.

Next, we determined the impact of testosterone, DHT, and estradiol on depot-specific fat mass expansion. Notably, testosterone treatment significantly reduced visceral and subcutaneous fat mass, and DHT reduced subcutaneous fat mass (Figure 3E,G). The DHT-mediated reduction in subcutaneous fat was not sufficient to reduce total fat mass compared with vehicle-treated castrated mice (Figure 3B). By contrast, estradiol treatment specifically reduced visceral fat expansion (Figure 3E), with no significant effect on subcutaneous fat mass (Figure 3G). Consistent with these findings, inhibition of aromatase activity in gonadally intact male animals resulted in the preferential accumulation of visceral fat (Figure 3J) and a more prominent visceral fat mass bias than in vehicle-treated gonadally intact males (Figure 3L). This effect on fat distribution is corroborated by the observation that estradiol reduces the proportion of visceral fat relative to subcutaneous fat in castrated mice (Figure 3I).

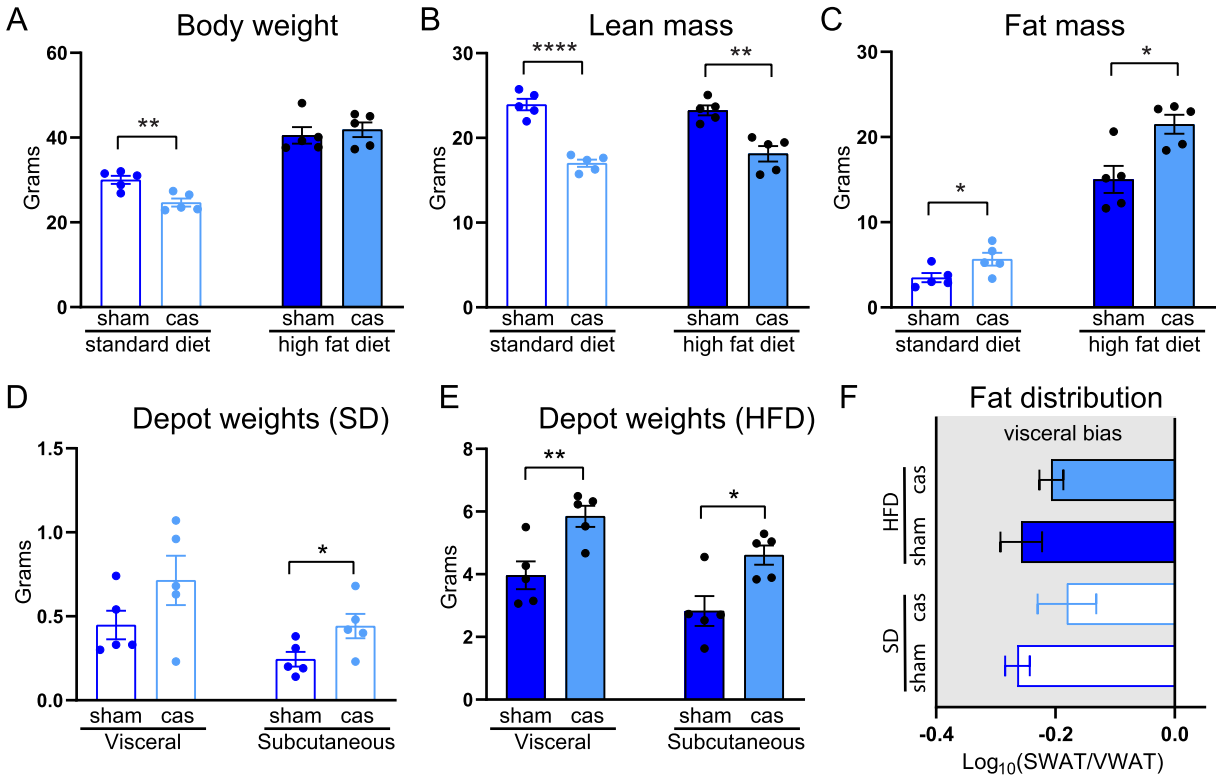

Figure 1: Castration alters body composition but not fat distribution. (A) Bodyweight. (B) Lean mass. (C) Fat mass. (D) Depot weights on a standard diet. (E) Depot weights on a high-fat diet. (F) Fat distribution. SD = standard diet, HFD = high-fat diet, SWAT = subcutaneous white adipose tissue, VWAT = visceral white adipose tissue. Statistical tests were unpaired Student's t tests between denoted groups.

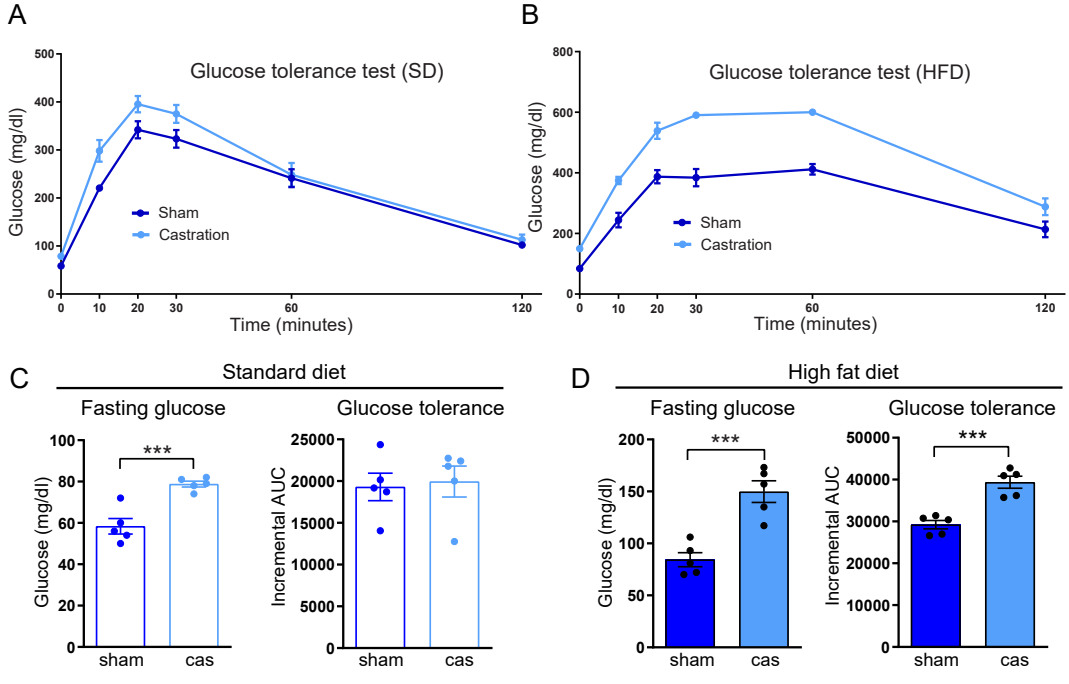

Figure 2: Male hypogonadism impairs glucose metabolism. (A) GTT curve for sham and castrated mice fed a standard diet (SD). (B) GTT curve for sham and castrated mice fed a high-fat diet (HFD). (C) Fasting glucose and glucose tolerance on an SD. (D) Fasting glucose and glucose tolerance on an HFD. Statistical tests in (C) and (D) were unpaired Student's *t* tests.

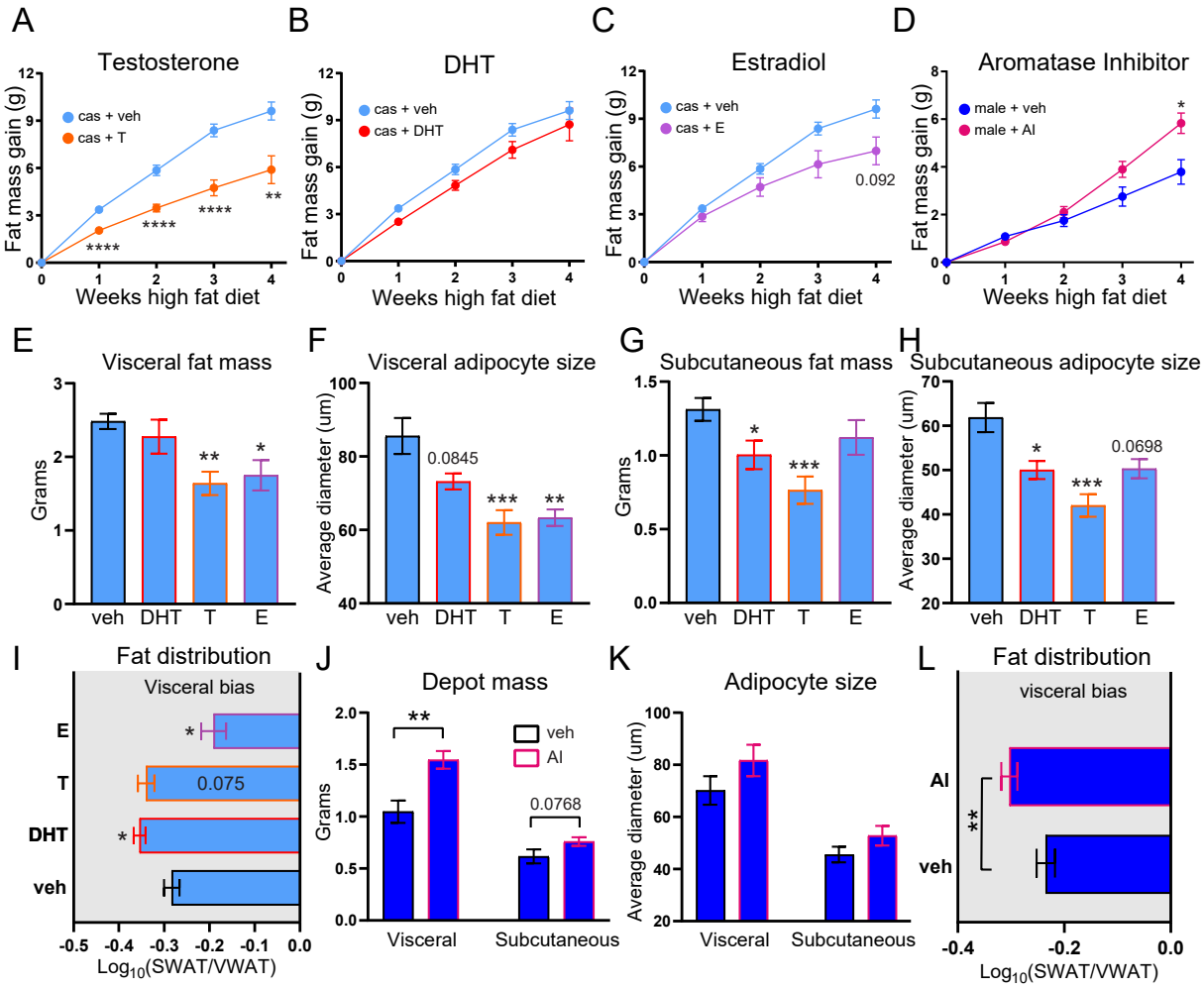

Figure 3: Testosterone metabolism incurs depot specificity to adipocyte hypertrophy. (A) Fat mass gain in castrated mice treated with vehicle or T on an HFD (n = 9–16). (B) Fat mass gain in castrated mice treated with vehicle or DHT on an HFD (n = 10–16). (C) Fat mass gain in castrated mice treated with vehicle or estradiol on an HFD (n = 5–16). (D) Fat mass gain in gonadally intact male mice treated with vehicle or aromatase inhibitor on an HFD (n = 14–15). (E) Visceral fat mass in castrated animals (n = 5–16). (F) Visceral adipocyte size in castrated animals (n = 5–16). (G) Subcutaneous fat mass in castrated animals (n = 5–16). (H) Subcutaneous adipocyte size in castrated animals (n = 5–16). (I) Fat distribution in castrated animals (n = 5–16). (J) Visceral and subcutaneous fat mass in vehicle- and aromatase inhibitor-treated male mice (n = 14–15). (K) Adipocyte size in visceral and subcutaneous fat of vehicle- and aromatase inhibitor-treated male mice (n = 14–15). (L) Fat distribution in male mice with and without aromatase inhibitor treatment (n = 14–15). Statistical significance in (A–D) was determined by using repeated measures two-way ANOVA with a Greenhouse-Geisser correction and Sidak's multiple comparisons test. Notably, the vehicle control is the same in (A–C); data were split into three graphs to aid visualization. Significance in (E–I) was determined by using one-way ANOVA. In (J–L) significance was determined by using unpaired Student's *t* tests.

Fat mass expansion occurs by the generation of new adipocytes (hyperplasia) and by the enlargement of existing adipocytes through lipid uptake (hypertrophy). Obesogenic adipocyte hyperplasia takes approximately 8 weeks from the outset of HFD feeding [37,47]. Significant changes in adipocyte size can occur in as little as 24 h [48,49]. Thus, because of the 4-week duration of these experiments, adipocyte hypertrophy is the most likely mechanism by which alterations in fat mass would occur. The depot-specific effects of testosterone, DHT, and estradiol on fat mass can be largely explained by changes in adipocyte size in castrated animals (Figure 3F,H; Supp. Fig. 1E). However, in male mice treated with AI, adipocyte size was only modestly elevated in visceral and subcutaneous fat (Figure 3K; Supp. Fig. 1F). As DHT reduced adipocyte size without affecting total fat mass in castrated mice, the subtle effects on adipocyte size in AI-treated animals could reflect the combined effects of reduced estradiol and elevated androgen activity.

3.3. Testosterone negatively regulates obesogenic adipogenesis in vivo in an AR-dependent manner

Enhanced adipocyte hyperplasia may also contribute to the increased fat mass observed in male hypogonadism. Adipocyte hyperplasia occurs through the proliferation and subsequent differentiation of APs. Importantly, this process is initiated by HFD feeding and AP proliferation occurs only during the first week of the HFD stimulus. Proliferative APs then differentiate into adipocytes over the next 7 weeks of HFD feeding. Therefore, AP proliferation, detectable after 1 week of HFD, can be used as a proxy for new adipocyte formation. Adipogenesis can also be directly assessed after 8 weeks of HFD feeding by using pulse-chase experiments that permanently label APs during proliferation [37].

We observed that basal AP proliferation on an SD was modestly higher in sham mice than in castrated mice (Supp. Fig. 2A), suggesting the increased fat mass in castrated mice on an SD is not due to adipocyte

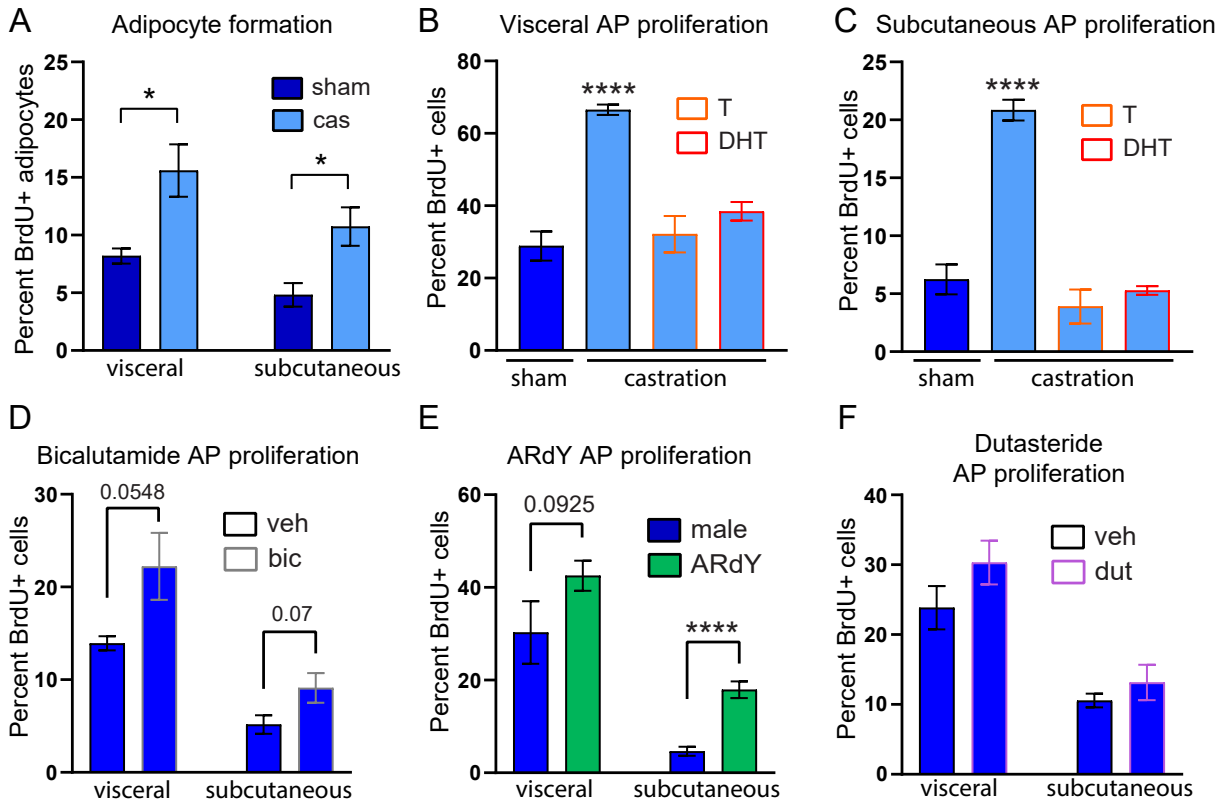

Figure 4: Androgen signaling negatively regulates obesogenic adipogenesis in vivo. (A) HFD-induced new adipocyte formation. (B) HFD-induced visceral adipocyte precursor proliferation. (C) HFD-induced subcutaneous adipocyte precursor proliferation. (D) HFD-induced adipocyte precursor proliferation upon low dose AR inhibitor treatment (25-30% recommended dose of bicalutamide for men with AR-dependent advanced stage prostate cancer). (E) HFD-induced adipocyte precursor proliferation in AR mutant mice. (F) HFD-induced adipocyte precursor proliferation in male mice treated with 5α-reductase inhibitor. Unpaired Student's t tests were performed in (A) and (D—F). Significance in (B, C) was determined by using one-way ANOVA and compared with the sham control.

hyperplasia. However, in response to HFD, obesogenic adipogenesis was enhanced in the visceral and subcutaneous fat of castrated mice relative to sham controls (Figure 4A), indicating hypogonadism increases susceptibility to adipogenesis in response to dietary fat intake. Consistent with these results, we observed that AP proliferation was significantly elevated in response to HFD in both fat depots, compared with sham controls (Figure 4B,C). Notably, treating castrated mice with either testosterone or DHT rescues the hyperproliferative response of APs to the HFD in castrated mice (Figure 4B,C). Given that DHT cannot be aromatized to estradiol, these data indicate that androgens, rather than estradiol, are sufficient to mediate anti-adipogenic effects in vivo and do so in an AR-dependent manner. Thus, we focused on the role of the androgen signaling pathway in this process.

We treated wildtype male mice with a low dose of the AR inhibitor, bicalutamide, and observed a modest elevation in AP proliferation in visceral and subcutaneous fat in response to an HFD (Figure 4D), without effects on seminal vesicle mass (Supp. Figure 2B). These data support the notion that AR activity negatively regulates HFD-induced AP proliferation. We also tested HFD-induced AP proliferation in mice without functional AR. These mice were karyotypically male (XY chromosomes) but developed female secondary sexual characteristics and ambiguous reproductive organs because of a deleterious mutation in the AR gene [31]. AR deficient XY (ARdY) mice exhibited enhanced HFD-induced AP proliferation, specifically in subcutaneous fat (Figure 4E). The reason for this depot specificity in ARdY mice is unclear. However, it has been suggested that the developmental establishment of visceral fat is impaired in ARdY mice [16], which could contribute to the dampened hyperproliferative response of this depot to an HFD. Altogether, these data support the conclusion that androgens negatively regulate adipogenesis in vivo in a manner dependent on AR function.

Next, we attempted to determine whether the anti-adipogenic effects of androgens are dependent on adipose-intrinsic AR function. To achieve this objective, we first profiled the mRNA expression of AR in a panel of several major organs and observed that AR is expressed in white adipose tissue at levels comparable to organs known to be highly sensitive to androgens such as the seminal vesicles and skeletal muscle (Supp. Fig. 2C). By digesting adipose tissue with collagenase, we separated adipocytes from stromal vascular cells and profiled AR expression in these different adipose-resident cell populations. Notably, AR expression was significantly greater in adipocytes than in total SVCs (Supp. Fig. 2D). Because multiple cell types compose the SVC population, high AR expression in one cell type might be masked by low AR expression in other SVCs. Therefore, we compared AR expression in isolated APs with whole SVCs and isolated CD45+ hematopoietic cells from adipose tissue. AR expression was significantly higher in APs than in whole SVCs and CD45+ cells (Supp. Fig. 2E). Thus, the adipocyte lineage is likely highly sensitive to androgens. To determine if AR function was required in APs for the anti-adipogenic effect of androgens, we transplanted mTomato+ APs from ARdY:mTmG mice, which have significantly reduced AR expression and function (Supp. Fig. 2F) [50], into wildtype male subcutaneous fat

and quantified HFD-induced AP proliferation. This strategy allowed us to differentiate AR mutant cells (mTomato+) from endogenous wild-type cells (no fluorescence). Surprisingly, ARdY:mTmG APs did not proliferate at a greater rate than endogenous male APs (Supp. Fig. 2G), suggesting that AR function in APs is not required for the anti-adipogenic effect of androgens in subcutaneous fat.

Lastly, we attempted to identify the physiologic ligand of AR required for its anti-adipogenic effect. If DHT was the major agonist of AR responsible for blocking adipogenesis, we would predict that reducing DHT levels in male mice would exacerbate HFD-induced adipogenesis. To test this hypothesis, we treated wildtype male mice with dutasteride, a pan 5a-reductase inhibitor [51] that blocks the conversion of testosterone to DHT. Dutasteride treatment significantly reduced seminal vesicle weight (Supp. Fig. 2H), indicating an effective reduction of DHT levels. Still, no effect was observed on HFD-induced AP proliferation compared with vehicle-treated males (Figure 4F). Thus, the major physiologic ligand of AR that negatively regulates adipogenesis in vivo is probably testosterone, not DHT.

4. DISCUSSION

Alterations in sex hormones have been associated with changes in body composition, fat distribution, and metabolic disease. However, the cellular mechanisms and adipose depot-specific effects of testosterone and its metabolites have been poorly described in vivo. In this study, we demonstrated that testosterone has potent anti-obesogenic effects. Notably, testosterone blocks the expansion of both visceral and subcutaneous fat (Figure 3E,G), and DHT specifically impedes subcutaneous fat growth (Figure 3E,G) without significantly impacting total fat mass (Figure 3B). Estradiol specifically prevents the expansion of visceral fat (Figure 3E,G). Thus, the conversion of testosterone to DHT and estradiol probably contributes to the regulation of depot-specific fat mass. The observation that estradiol preferentially impedes visceral fat expansion in diet-induced obesity is particularly intriguing because men are more likely to develop visceral obesity than women are [52–54]. It is possible that comparatively reduced estrogen signaling promotes visceral fat mass expansion without significantly impacting subcutaneous fat storage, which could contribute not only to visceral obesity in men but in post-menopausal women. Consistent with this notion, ovariectomized mice display markedly enhanced visceral adipogenesis and are more prone to visceral obesity when fed an HFD [55,56].

Fat mass is a function of adipocyte size and adipocyte number [57]. We demonstrated that in castrated mice, hormone-dependent changes in depot-specific fat mass reflect concomitant changes in adipocyte size (Figure 3E–H). However, in gonadally intact male mice treated with AI, depot-specific changes in fat mass did not reflect changes in adipocyte size (Figure 3J,K). A possibility is that this discrepancy occurs because of the relatively brief (4 weeks) duration of the experiment, as gonadally intact male mice gain less fat mass on an HFD than castrated mice do, even when treated with AI (Figure 3A–D). Thus, a longer duration of HFD feeding and AI treatment (and greater fat gain) may be required to reveal differences in adipocyte size that reflect the elevated visceral fat in these animals. In addition, elevated androgen activity in AI-treated males may obscure the effects on visceral adipocyte hypertrophy by estradiol loss. Regardless, these data support the notion that testosterone, DHT, and estradiol exert unique effects on depot-specific adipocyte hypertrophy but likely act in combination under normal physiologic conditions. In this study, mice were castrated before puberty to control for hormonal alterations that occur during this life stage. Determining the individual contributions of sex hormones to the regulation of total adiposity and fat distribution at different life stages will be an important area of further investigation.

We also assessed the role of androgens in obesogenic adipogenesis. Notably, castration resulted in elevated HFD-induced new adipocyte formation in visceral and subcutaneous fat (Figure 4A), indicating hypogonadism increases susceptibility to obesogenic adipogenesis when dietary fat intake is high. Treating castrated mice with either testosterone or DHT completely rescued this effect (Figure 4B,C), which was surprising due to the inability of DHT to reduce total fat mass gain on an HFD (Figure 3B). However, inhibiting 5α-reductase activity in gonadally intact male mice had no impact on HFD-induced AP proliferation (Figure 4F), suggesting testosterone rather than DHT is the major agonist of AR that inhibits adipogenesis in vivo. We also showed that AR is highly expressed in APs (Supp. Fig. 2E) and mature adipocytes (Supp. Fig. 2D) but that the anti-adipogenic effect of androgens appears not to require AP-intrinsic AR function (Supp. Fig. 2G). This finding is in contrast to the work in vitro with adipogenic cell lines [12,14]. Further work is necessary to identify how AR blocks adipogenesis in vivo but may involve crosstalk with mature adipocytes or systemic effects of androgens. Characterizing the cellular contexts in which testosterone metabolism is required to control obesogenic adipogenesis and depot-specific fat mass will be important next steps in understanding the role of sex hormones in the pathogenesis of obesity and its related metabolic diseases.

ACKNOWLEDGMENTS

The authors thank Michael Schadt and the Yale Comparative Medicine Histology Core for assistance in sectioning and staining adipose tissue samples. We also thank Zhao Zhao and the Yale Flow Cytometry Core for the use of their facilities and technical expertise in cell sorting. This work was funded by a National Science Foundation Graduate Research Fellowship (DGE1122492 to Z.L.S.) and by the NIDDK (R01DK110147 and DK090489 to M.S.R.).

CONFLICT OF INTEREST

None declared.

APPENDIX A. SUPPLEMENTARY DATA

Supplementary data to this article can be found online at https://doi.org/10.1016/j.molmet.2020.101141.

REFERENCES

[1] Bojesen, A., Høst, C., Gravholt, C.H., 2010. Klinefelter's syndrome, type 2 diabetes and the metabolic syndrome: the impact of body composition. MHR: Basic Science of Reproductive Medicine 16(6):396–401.

[2] Brodsky, I.G., Balagopal, P., Nair, K.S., 1996. Effects of testosterone replacement on muscle mass and muscle protein synthesis in hypogonadal men-a clinical research center study. Journal of Clinical Endocrinology & Metabolism 81(10):3469–3475.

[3] Mulligan, T., Frick, M., Zuraw, Q., Stemhagen, A., McWhirter, C., 2006. Prevalence of hypogonadism in males aged at least 45 years: the HIM study. International Journal of Clinical Practice 60(7):762–769.

[4] Bojesen, A., Kristensen, K., Birkebaek, N.H., Fedder, J., Mosekilde, L., Bennett, P., et al., 2006. The metabolic syndrome is frequent in Klinefelter's syndrome and is associated with abdominal obesity and hypogonadism. Diabetes Care 29(7):1591–1598.

[5] Mrin, P., Arver, S., 1998. Androgens and abdominal obesity. Baillière's Clinical Endocrinology and Metabolism 12(3):441–451.

[6] Seidell, J.C., Björntorp, P., Sjöström, L., Kvist, H., Sannerstedt, R., 1990. Visceral fat accumulation in men is positively associated with insulin, glucose, and C-peptide levels, but negatively with testosterone levels. Metabolism 39(9):897–901.

[7] Griggs, R.C., Kingston, W., Jozefowicz, R.F., Herr, B.E., Forbes, G., Halliday, D., 1989. Effect of testosterone on muscle mass and muscle protein synthesis. Journal of Applied Physiology 66(1):498–503.

[8] O'Connell, M.D., Wu, F.C., 2014. Androgen effects on skeletal muscle: implications for the development and management of frailty. Asian Journal of Andrology 16(2):203.

[9] Bhasin, S., Jasuja, R., 2009. Selective androgen receptor modulators (SARMs) as function promoting therapies. Current Opinion in Clinical Nutrition and Metabolic Care 12(3):232.

[10] Durdiakova, J., Ostatnikova, D., Celec, P., 2011. Testosterone and its metabolites—modulators of brain functions. Acta Neurobiologiae Experimentalis.

[11] Prossnitz, E.R., Arterburn, J.B., Smith, H.O., Oprea, T.I., Sklar, L.A., Hathaway, H.J., 2008. Estrogen signaling through the transmembrane G protein–coupled receptor GPR30. Annual Review of Physiology 70:165–190.

[12] Singh, R., Artaza, J.N., Taylor, W.E., Gonzalez-Cadavid, N.F., Bhasin, S., 2003. Androgens stimulate myogenic differentiation and inhibit adipogenesis in C3H 10T1/2 pluripotent cells through an androgen receptor-mediated pathway. Endocrinology 144(11):5081–5088.

[13] Gupta, V., Bhasin, S., Guo, W., Singh, R., Miki, R., Chauhan, P., et al., 2008. Effects of dihydrotestosterone on differentiation and proliferation of human mesenchymal stem cells and preadipocytes. Molecular and Cellular Endocrinology 296(1–2):32–40.

[14] Singh, R., Artaza, J.N., Taylor, W.E., Braga, M., Yuan, X., Gonzalez-Cadavid, N.F., et al., 2006. Testosterone inhibits adipogenic differentiation in 3T3-L1 cells: nuclear translocation of androgen receptor complex with β-catenin and T-cell factor 4 may bypass canonical Wnt signaling to down-regulate adipogenic transcription factors. Enfdocrinology 147(1):141–154.

[15] Mårin, P., Holmtäng, S., Gustafsson, C., Jönsson, L., Kvist, H., Elander, A., et al., 1993. Androgen treatment of abdominally obese men. Obesity Research 1(4):245–251.

[16] Dubois, V., Laurent, M.R., Jardi, F., Antonio, L., Lemaire, K., Goyvaerts, L., et al., 2016. Androgen deficiency exacerbates high-fat diet-induced metabolic alterations in male mice. Endocrinology 157(2):648–665.

[17] Sato, T., Matsumoto, T., Yamada, T., Watanabe, T., Kawano, H., Kato, S., 2003. Late onset of obesity in male androgen receptor-deficient (AR KO) mice. Biochemical and Biophysical Research Communications 300(1):167–171.

[18] Movérare-Skrtic, S., Venken, K., Andersson, N., Lindberg, M.K., Svensson, J., Swanson, C., et al., 2006. Dihydrotestosterone treatment results in obesity and altered lipid metabolism in orchidectomized mice. Obesity 14(4):662–672.

[19] Dakin, R.S., Walker, B.R., Seckl, J.R., Hadoke, P.W., Drake, A.J., 2015. Estrogens protect male mice from obesity complications and influence glucocorticoid metabolism. International Journal of Obesity 39(10):1539–1547.

[20] Ohlsson, C., Hellberg, N., Parini, P., Vidal, O., Bohlooly, M., Rudling, M., et al., 2000. Obesity and disturbed lipoprotein profile in estrogen receptor-α-deficient male mice. Biochemical and Biophysical Research Communications 278(3):640–645.

[21] Jones, M.E., Thorburn, A.W., Britt, K.L., Hewitt, K.N., Misso, M.L., Wreford, N.G., et al., 2001. Aromatase-deficient (ArKO) mice accumulate excess adipose tissue. The Journal of Steroid Biochemistry and Molecular Biology 79(1–5):3–9.

[22] Jones, M.E., Thorburn, A.W., Britt, K.L., Hewitt, K.N., Wreford, N.G., Proietto, J., et al., 2000. Aromatase-deficient (ArKO) mice have a phenotype of increased adiposity. Proceedings of the National Academy of Sciences 97(23):12735–12740.

[23] Maffei, L., Murata, Y., Rochira, V., Tubert, G., Aranda, C., Vazquez, M., et al., 2004. Dysmetabolic syndrome in a man with a novel mutation of the aromatase gene: effects of testosterone, alendronate, and estradiol treatment. Journal of Clinical Endocrinology & Metabolism 89(1):61–70.

[24] Lemieux, S., Prud'homme, D., Bouchard, C., Tremblay, A., Després, J.-P., et al., 1993. Sex differences in the relation of visceral adipose tissue accumulation to total body fatness. American Journal of Clinical Nutrition 58(4):463–467.

[25] Ley, C.J., Lees, B., Stevenson, J.C., 1992. Sex-and menopause-associated changes in body-fat distribution. American Journal of Clinical Nutrition 55(5):950–954.

[26] Reubinoff, B.E., Wurtman, J., Rojansky, N., Adler, D., Stein, P., Schenker, J.G., et al., 1995. Effects of hormone replacement therapy on weight, body composition, fat distribution, and food intake in early postmenopausal women: a prospective study. Fertility and Sterility 64(5):963–968.

[27] Boyanov, M., Boneva, Z., Christov, V., 2003. Testosterone supplementation in men with type 2 diabetes, visceral obesity and partial androgen deficiency. The Aging Male 6(1):1–7.

[28] Kapoor, D., Boneva, Z., Christov, V., 2006. Testosterone replacement therapy improves insulin resistance, glycaemic control, visceral adiposity and hypercholesterolaemia in hypogonadal men with type 2 diabetes. European Journal of Endocrinology 154(6):899–906.

[29] Frederiksen, L., Højlund, K., Hougaard, D., Mosbech, T.H., Larsen, R., Flyvbjerg, A., et al., 2012. Testosterone therapy decreases subcutaneous fat and adiponectin in aging men. European Journal of Endocrinology 166(3):469.

[30] Katznelson, L., Finkelstein, J.S., Schoenfeld, D.A., Rosenthal, D.I., Anderson, E.J., Klibanski, A., 1996. Increase in bone density and lean body mass during testosterone administration in men with acquired hypogonadism. Journal of Clinical Endocrinology & Metabolism 81(12):4358–4365.

[31] Lyon, M.F., Hawkes, S.G., 1970. X-linked gene for testicular feminization in the mouse. Nature 227(5264):1217–1219.

[32] Muzumdar, M.D., et al., 2007. A global double-fluorescent Cre reporter mouse. Genesis 45(9):593–605.

[33] Tyrrell, C., Kaisary, A., Iversen, P., Anderson, J., Baert, L., Tammela, T., et al., 1998. A randomised comparison of 'Casodex'TM (bicalutamide) 150 mg monotherapy versus castration in the treatment of metastatic and locally advanced prostate cancer. European Urology 33(5):447–456.

[34] McLeod, D.G., Iversen, P., See, W.A., Morris, T., Armstrong, J., Wirth, M.P., et al., 2006. Bicalutamide 150 mg plus standard care vs standard care alone for early prostate cancer. BJU International 97(2):247–254.

[35] Berry, R., Church, C.D., Gericke, M.T., Jeffery, E., Colman, L., Rodeheffer, M.S., 2014. Imaging of adipose tissue. In: Methods in enzymology. Elsevier. p. 47–73.

[36] Carpenter, A.E., Jones, T.R., Lamprecht, M.R., Clarke, C., Kang, I.H., Friman, O., et al., 2006. CellProfiler: image analysis software for identifying and quantifying cell phenotypes. Genome Biology 7(10):R100.

[37] Jeffery, E., Church, C.D., Holtrup, B., Colman, L., Rodeheffer, M.S., 2015. Rapid depot-specific activation of adipocyte precursor cells at the onset of obesity. Nature Cell Biology 17(4):376–385.

[38] Katsuno, M., Adachi, H., Kume, A., Li, M., Nakagomi, Y., Niwa, H., et al., 2002. Testosterone reduction prevents phenotypic expression in a transgenic mouse model of spinal and bulbar muscular atrophy. Neuron 35(5):843–854.

[39] Christoffersen, B.O., Gade, L.P., Golozoubova, V., Svendsen, O., Raun, K., 2010. Influence of castration-induced testosterone and estradiol deficiency on obesity and glucose metabolism in male Göttingen minipigs. Steroids 75(10):676–684.

[40] Aoki, A., Fujitani, K., Takagi, K., Kimura, T., Nagase, H., Nakanishi, T., 2016. Male hypogonadism causes obesity associated with impairment of hepatic gluconeogenesis in mice. Biological and Pharmaceutical Bulletin 39(4):587–592.

[41] Klip, A., Pâquet, M.R., 1990. Glucose transport and glucose transporters in muscle and their metabolic regulation. Diabetes Care 13(3):228—243.

[42] Brooks, N., Layne, J.E., Gordon, P.L., Roubenoff, R., Nelson, M.E., Castaneda-Sceppa, C., 2007. Strength training improves muscle quality and insulin sensitivity in Hispanic older adults with type 2 diabetes. International Journal of Medical Sciences 4(1):19.

[43] Atlantis, E., Martin, S.A., Haren, M.T., Taylor, A.W., Wittert, G.A., 2009. Inverse associations between muscle mass, strength, and the metabolic syndrome. Metabolism 58(7):1013—1022.

[44] Srikanthan, P., Karlamangla, A.S., 2011. Relative muscle mass is inversely associated with insulin resistance and prediabetes. Findings from the third National Health and Nutrition Examination Survey. Journal of Clinical Endocrinology & Metabolism 96(9):2898—2903.

[45] Mokdad, A.H., Ford, E.S., Bowman, B.A., Dietz, W.H., Vinicor, F., Bales, V.S., et al., 2001. Prevalence of obesity, diabetes, and obesity-related health risk factors. Jama 289(1):76—79, 2003.

[46] Guise, T.A., Oefelein, M.G., Eastham, J.A., Cookson, M.S., Higano, C.S., Smith, M.R., 2007. Estrogenic side effects of androgen deprivation therapy. Reviews in Urology 9(4):163.

[47] Wang, Q.A., Tao, C., Gupta, R.K., Scherer, P.E., 2013. Tracking adipogenesis during white adipose tissue development, expansion and regeneration. Nature Medicine 19(10):1338—1344.

[48] Sun, K., Kusminski, C.M., Scherer, P.E., 2011. Adipose tissue remodeling and obesity. Journal of Clinical Investigation 121(6):2094—2101.

[49] Halberg, N., Khan, T., Trujillo, M.E., Wernstedt-Asterholm, I., Attie, A.D., Sherwani, S., et al., 2009. Hypoxia-inducible factor 1α induces fibrosis and insulin resistance in white adipose tissue. Molecular and Cellular Biology 29(16):4467—4483.

[50] Charest, N.J., Zhou, Z.-X., Lubahn, D.B., Olsen, K.L., Wilson, E.M., French, F.S., 1991. A frameshift mutation destabilizes androgen receptor messenger RNA in the Tfm mouse. Molecular Endocrinology 5(4):573—581.

[51] Yamana, K., Labrie, F., 2010. Human type 3 5α-reductase is expressed in peripheral tissues at higher levels than types 1 and 2 and its activity is potently inhibited by finasteride and dutasteride. Hormone Molecular Biology and Clinical Investigation 2(3):293—299.

[52] Palmer, B.F., Clegg, D.J., 2015. The sexual dimorphism of obesity. Molecular and Cellular Endocrinology 402:113—119.

[53] Palmisano, B.T., Zhu, L., Eckel, R.H., Stafford, J.M., 2018. Sex differences in lipid and lipoprotein metabolism. Molecular metabolism 15:45—55.

[54] Santosa, S., Hensrud, D.D., Votruba, S.B., Jensen, M.D., 2008. The influence of sex and obesity phenotype on meal fatty acid metabolism before and after weight loss. American Journal of Clinical Nutrition 88(4):1134—1141.

[55] Stubbins, R.E., Holcomb, V.B., Hong, J., Núñez, N.P., 2012. Estrogen modulates abdominal adiposity and protects female mice from obesity and impaired glucose tolerance. European Journal of Nutrition 51(7):861—870.

[56] Jeffery, E., Wing, A., Holtrup, B., Sebo, Z., Kaplan, J.L., Saavedra-Peña, R., et al., 2016. The adipose tissue microenvironment regulates depot-specific adipogenesis in obesity. Cell Metabolism 24(1):142—150.

[57] Jo, J., Gavrilova, O., Pack, S., Jou, W., Mullen, S., Sumner, A.E., et al., 2009. Hypertrophy and/or hyperplasia: dynamics of adipose tissue growth. PLoS Computational Biology 5(3):e1000324.

